# Superparamagnetic Blocking of an Ensemble of Magnetite Nanoparticles upon Interparticle Interactions

D.A. Balaev[1,2], S.V. Semenov[1,2], A.A. Dubrovskiy[1], S.S. Yakushkin[3,4], V.L. Kirillov[3], O.N. Martyanov[3,4].

[1] – Kirensky Institute of Physics, Federal Research Center KSC SB RAS, Krasnoyarsk, 660036, Russia

[2] – Siberian Federal University, Krasnoyarsk, 660041, Russia

[3] – Boreskov Institute of Catalysis, Novosibirsk, 630090, Russia

[4] – Novosibirsk State University, Novosibirsk, 630090, Russia

**Abstract—**We report on the effect of interparticle magnetic interactions in an ensemble of superparamagnetic magnetite particles with an average size of ~8.4 nm dispersed in the diamagnetic matrix on the blocking of this ensemble in external magnetic field. The two limit cases are investigated: the case of strongly interacting particles, when the value of magnetic dipole-dipole interaction between particles is comparable with the energy of other interactions in the ensemble (the interparticle distance is similar to the nanoparticle diameter) and the case of almost noninteracting particles distant from each other by about ten particle diameters. We demonstrate that the experimental dependence of the blocking temperature on external field is described well within the model [1], in which the density of particles in a nonmagnetic medium is taken into account and the correlation value depends on external magnetic field. The model for describing the magnetic properties of a disperse nanoparticle ensemble is proposed, which makes corrections related to the particle size and mean dipole-dipole interaction energy for the anisotropy constant. The surface magnetic anisotropy of $Fe_3O_4$ particles and parameters of the interparticle coupling are estimated.

**Keywords:** $Fe_3O_4$ nanoparticles; superparamagnetic nanoparticles; size effect; blocking temperature.



## 1. Introduction

The range of possible applications of magnetic nanoparticles has been permanently broadening and currently involves biomedicine (drug transport, diagnostics, imprinted polymers, and hyperthermia) [2] high-density magnetic memory [3–7], catalysis [8–10], etc.

In the overwhelming majority of the problems to be solved, researches and engineers deal not with isolated particles, but with their ensembles. Therefore, along with the fundamental problem of forming nanoparticles of specified sizes, surface properties, and magnetic characteristics, there exists the equally important problem that concerns the effect of interparticle magnetic interactions on the magnetic properties of ensembles of interacting particles [11–14]. The magnetic interparticle interactions can significantly change the magnetization, coercivity, and other magnetic characteristics of an ensemble and give rise to various effects, which are not averaged even over a sufficiently large ensemble of magnetic particles [15–17] Thus, when describing the magnetic properties of interacting nanoparticles, even with taking account for only dipole-dipole interactions, we should consider not only the standard characteristics (volume and surface magnetic anisotropy, size distribution of particles, and temperature of the transition to the blocked state), but also parameters of the interaction between magnetic particles [1,18–22].

In particular, an urgent problem is the transition of an ensemble of single-domain superparamagnetic nanoparticles to the so-called blocked state upon magnetic coupling between them. The temperature $T_B$ of superparamagnetic blocking of noninteracting particles is determined using the well-known Neel–Brown formula

$$T_B = \frac{K_{eff} V}{k_B \ln(\tau / \tau_0)} \quad (1)$$

where $K_{eff}$ is the effective magnetic anisotropy constant consisting of the volume ($K_V$) and surface ($6K_S/d$, where $d$ is the linear particle size) contributions, $V$ is the particle volume, $k_B$ is the Boltzmann constant, $\tau$ is the characteristic measuring time and $\tau_0$ is the particle relaxation time ($\tau_0 \sim 10^{-9}$–$10^{-11}$ s). In the quasi-static magnetic measurements ($\tau \sim 10^{1-2}$ s) discussed here, Eq. (1) yields $T_B \approx K_{eff}V/25k_B$.

In the presence of the interactions, one can observe an increase in the blocking temperature [1,12–14,18–20], which can be reduced to the additional contribution to $K_{eff}$ proportional to the interaction energy $U_{int}$:

$$T_B = \frac{(K_V + 6K_S / d)V + U_{int}}{k_B \ln(\tau / \tau_0)} \quad (2)$$

However, it is fairly difficult to interpret the field dependence of the blocking temperature within this approach, since Eqs. (1) and (2) are applicable, strictly speaking, only for weak external magnetic fields. The approach to the description of the $T_B(H)$ dependence in the presence of interparticle interactions developed in [1,18] made it possible to unambiguously interpret the experimental data on Co-$SiO_2$ granular films [1] and two-dimensional $Fe_3O_4$ film systems [18]. It seems reasonable to extend these investigations to three-dimensional systems, in which nanoparticles are spatially stabilized but separated by distances of several linear particle sizes.

Lately, we proposed an original technique for fabricating $Fe_3O_4$ magnetite nanoparticles with the use of citrate-ion agents blocking the particle growth. Using our technique, particles with an average size of 4–10 nm and a narrow size distribution can be controllably formed [23]. In this work, we investigate samples of nanoparticles with an average size of $\langle d \rangle \approx 8.4$ nm prepared using this technique and dispersed in paraffin in concentrations of ~0.25 and ~38 wt.% to ensure spatial stabilization. At $\langle d \rangle \approx 8.4$ nm, these two concentrations correspond to the average interparticle distances of about one and ten $\langle d \rangle$ values. The main focus of the current work is the dependence of the blocking temperature of these systems on external magnetic field.

## 2. Experimental

$Fe_3O_4$ nanoparticles were formed by co-deposition of $Fe^{2+}$ and $Fe^{3+}$ ($[Fe^{3+}]/[Fe^{2+}] = 2$) salts from the aqueous solution by ammonium hydroxide in the presence of citrate ions using the technique described in [23].

High-resolution transmission electron microscopy (HR TEM) study was carried out on a JEOL JEM-2010 microscope at an accelerating voltage of 200 kV with resolution of 1.4 Å. The size distribution of nanoparticles was calculated using several photographs taken from different sample areas. The obtained product was dispersed in paraffin in magnetite concentrations of ~0.25 and ~38 wt.% (~0.044 and ~10 vol.%). Hereinafter, the samples are referred to as 0.044% $Fe_3O_4$ and 10% $Fe_3O_4$ in accordance with the magnetite volume concentration.

Magnetic measurements were performed on a vibrating sample magnetometer. Temperature dependences of the magnetic moment M(T) were measured upon zero-field cooling (ZFC mode) from room temperature and upon cooling in an external field (FC mode). The data obtained were corrected to the diamagnetic signal from paraffin.

## 3. Results and discussion

*3.1. Blocking temperature distribution and effective magnetic anisotropy constant for noninteracting particles*

For further analysis of the blocking temperature as a function of magnetic field $H$, it is necessary to determine the effective magnetic anisotropy constant $K_{eff}$ for magnetite nanoparticles upon weak interparticle interactions (sample 0.044% $Fe_3O_4$). Figure 1 shows the $M(T)_{ZFC}$ dependence for sample 0.044% $Fe_3O_4$ in a field of $H = 100$ Oe. The $M(T)_{ZFC}$ dependence for noninteracting particles in a sufficiently weak applied field can be described as [12,13]

$$\frac{M(T)}{H} = \frac{M_S^2}{3K_{eff}}\left[\ln\left(\frac{\tau}{\tau_0}\right)\int_0^T \frac{T_B}{T} f(T_B)dT_B + \int_T^\infty f(T_B)dT_B\right] \quad (3)$$

In Eq. (3), $M_S$ is the saturation magnetization of a particle and $f(T_B)$ is the blocking temperature distribution function.

It can be seen from Eqs. (1) and (2) that the blocking temperature of an isolated particle is directly proportional to its volume. As it is known from the literature [24], the size characteristics of nanoparticles during synthesis are described well by the lognormal distribution. Thus, we can use the lognormal distribution as a blocking temperature distribution function of particles, $f(T_B) = (T_B \cdot s \cdot (2\pi)^{1/2})^{-1} \exp\{-[\ln(T_B/n)]^2/2s^2\}$ with an average value of $\langle T_B \rangle = n \cdot \exp(s^2)$ and a dispersion of $\ln(T_B) = s^2$.

Substituting the obtained $f(T_B)$ value to Eq. (3) and varying the parameters $\langle T_B \rangle$ and $s^2$, we can obtain the best agreement of the $M(T)$ function from Eq. (3) with the experimental data. Figure 2 presents the results of the best fitting of the $M(T)_{ZFC}$ dependence (solid lines, the $Y$ axis is the right scale) and the $f(T_B)$ function (the $Y$ axis is the left scale). These results were obtained at $\langle T_B \rangle \approx 82$ K, $K_{eff} = 2.2 \times 10^5$ erg/cm$^3$, and $M_S \approx 92$ emu/g. Note that the obtained value $\langle T_B \rangle \approx 82$ K agrees well with the temperature $T_{max}$ at which the $M(T)_{ZFC}$ dependence has the maximum.

The obtained $f(T_B)$ dependence allows us to reproduce with good accuracy the shape of the size distribution function $f(d)$ using Eq. (1) with the above-mentioned parameters. Along with the particle size distribution histogram, Fig. 2 shows the $f(d)$ dependence, which is in good agreement with the HRTEM data. The value $K_{eff} = 2.2 \times 10^5$ erg/cm$^3$ is somewhat higher than $K_V \sim 1.1 \times 10^5$ erg/cm$^3$ [25,26] for bulk magnetite, which is explained by the effect of surface anisotropy. At $d = \langle d \rangle \approx 8.4$ nm, $K_S$ is ~0.015 erg/cm$^2$, which is consistent with the analogous estimates for $Fe_3O_4$ [25].

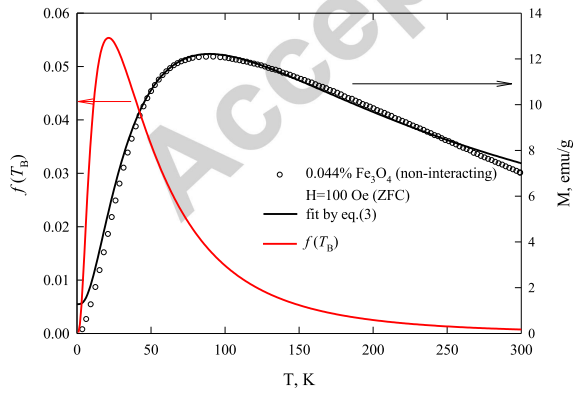


Fig.1.

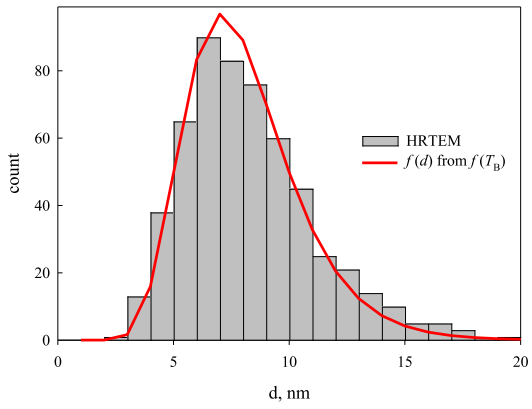


Fig. 2.

Fig. 1. Temperature dependence of magnetic moment $M(T)$ for sample 0.044% $Fe_3O_4$ (the Y axis is the right scale) in a field of $H = 100$ Oe and results of the best fitting by Eq.(3) with the distribution function $f(T_B)$ (the Y axis is the left scale).

Fig. 2. Particle size distribution histogram and distribution function $f(d)$ obtained from the $f(T_B)$ dependence in Fig. 1.

### *3.2. Field dependence of $T_{max}$*

Figure 3 shows the $M(T)$ dependences of the investigated samples obtained in the ZFC and FC modes in different external fields $H$. The $M(T)_{ZFC}$ dependences have the maximum at $T = T_{max}$, which shifts toward lower temperatures with increasing external field. The temperature of the irreversible behavior of the magnetization (ZFC and FC modes) is similar.

The dependences of $T_{max}$ on external field $H$ for the samples under study are presented in Fig. 4. It can be seen that in weak magnetic fields the dependences for two samples are essentially different. For sample 10% $Fe_3O_4$, $T_{max}$ increases sharper with decreasing external field than for sample 0.044% $Fe_3O_4$. This difference can be attributed to the higher energy of interparticle interactions in sample 10% $Fe_3O_4$.

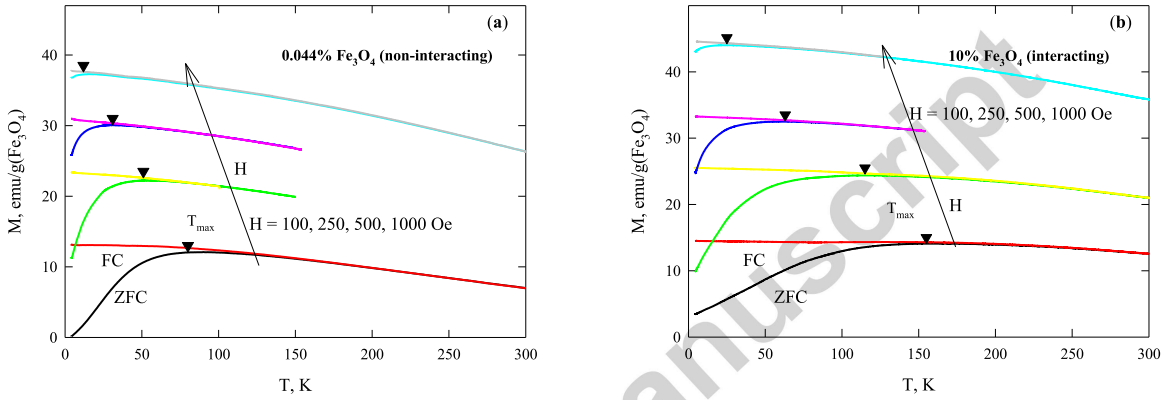


Fig. 3a, b.

Fig. 3. Temperature dependences of magnetic moment in different external fields and thermomagnetic prehistory of the investigated samples.

The field dependence of the blocking temperature for noninteracting particles is described by the classical relation

$$T_B(H) = \frac{K_{eff}V}{k_B \ln(\tau/\tau_0)}\left[1 - \frac{M_S H}{2K_{eff}}\right]^{3/2}. \quad (4)$$

In the case of noninteracting particles, we use a modified random anisotropy model (RAM) [27] developed in [1,18]. This model deals not with an isolated particle, but with a cluster of the larger size, which includes a certain number of particles depending on volume concentration $x$. The correlation length $L_H$ of such a cluster depends on the external field as

$$L_H = d + \sqrt{\frac{2A_{eff}}{M_S H + C}} \quad (5)$$

Here, $A_{eff}$ corresponds to the interparticle interaction intensity and has the meaning of volume constant and $C$ is responsible for the interaction intensity variation with particle concentration and plays an important role only in fields close to zero [1,18].

In this case, the anisotropy constant also changes as

$$K \to \frac{K}{\sqrt{N}} = \frac{K}{\sqrt{1+\frac{x(L_H^3 - d^3)}{d^3}}} \quad (6)$$

where $N$ is the number of particles in a cluster, which, in turn, can be expressed through the correlation length. As a result, the dependence of $T_B$ on $H$ (Eq. (4)) is transformed to

$$T_B(H) = \frac{K_{eff}\left[d^3 + x(L_H^3 - d^3)\right]}{6k_B \ln\left(\frac{\tau_m}{\tau_0}\right)\sqrt{1+\frac{x(L_H^3 - d^3)}{d^3}}} \times \left[1 - \frac{HM_S\sqrt{1+\frac{x(L_H^3 - d^3)}{d^3}}}{2K_{eff}}\right]^{\frac{3}{2}} \quad (7)$$

This expression is written for cubic particles ($V = d^3$).

Using the obtained dependence, we can simulate the experimental data (Fig. 4). The procedure suggests that the $M_S$ and $d$ values should be analogous for both samples due to the identity of the particle size distributions and the $K_{eff}$ values should agree well with the contribution of the surface anisotropy at the $K_S$ value obtained in Section 3.1.

Figure 4 shows the results of the simulation (lines) of the experimental data using Eq. (4) for sample 0.044% $Fe_3O_4$ and Eq. (7) for sample 10% $Fe_3O_4$. One can see the satisfactory agreement for the case of noninteracting particles and good agreement for the system with the interparticle coupling. The simulation parameters are given in Table 1.

Table 1. Parameters used in the simulation of the $T_{max}(H)$ dependences for the investigated samples

| Sample | $M_s$ emu/g | d nm | $K_{eff}$ erg/cm$^3$ | $K_s$ erg/cm$^2$ | $A_{eff}$ erg/cm$^{-1}$ |
|---|---|---|---|---|---|
| 0.044% $Fe_3O_4$ | 92 | 12 | $1.85\times10^5$ | 0.015 | -- |
| 10% $Fe_3O_4$ | 92 | 12 | $3.15\times10^5$ erg/cm$^3$ | 0.015 | $2\times10^{-8}$ ($x=0.1$) |

For sample 0.044% $Fe_3O_4$, the $K_{eff}$ value agrees well with the above estimate $K_S \approx 0.015$ erg/cm$^2$: $K_{bulk} + 6K_S/d \approx 1.85 \times 10^5$ erg/cm$^3$ at $d = 12$ nm. At this $K_{eff}$ value, the blocking temperature (Eq. (1)) for a particle 12 nm in size is ~84 K, which is similar to $T_{max} \approx 80$ K and $\langle T_B \rangle \approx 82$ K in the $f(T_B)$ dependence (Fig. 1) for the data obtained in a field of $H = 100$ Oe.

Using the $K_{eff}$ value for sample 10% $Fe_3O_4$, we can determine $U_{int}/k_B$ (Eq. (2)): $U_{int}/k_B = (3.15 - 1.85) \times 10^5$ erg/cm$^3$ $= 1.3 \times 10^5$ erg/cm$^3$. The $A_{eff}$ value obtained by fitting is larger than the value reported in [18]. This is apparently due to the different natures of the samples. In the work of M.Knobel [18], the magnetite particle size in the investigated sample was smaller (5.8 nm) and the sample was a nearly two-dimensional nanoparticle film. At the same time, the system under study was bulk, which should lead to an increase in the energy of interparticle coupling.

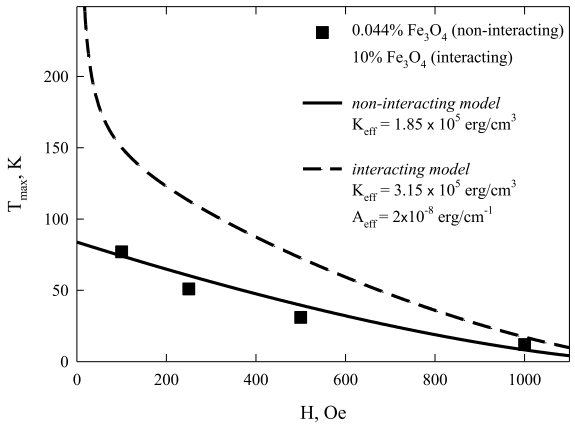


Fig. 4.

Fig. 4. Dependences of temperature $T_{max}$ of the $M(T)_{ZFC}$ curves (Fig. 3) for samples 0.044% $Fe_3O_4$ and10% $Fe_3O_4$ on external field $H$ (dots) and model dependences obtained using Eqs. (4) and (6) with the above-mentioned parameters (see Section 3.2).

## 4. Conclusions

The processes of magnetic blocking in magnetite nanoparticle ensembles were investigated. It was shown that the strong interparticle interactions lead to an increase in the temperature of the maximum in the $M(T)$ dependence (blocking temperature) and the temperature of irreversible behavior of the magnetization. The magnetic-field dependence of the blocking temperature upon interparticle interactions descends faster than the dependence for the sample with almost noninteracting particles. This dependence is described well using the model from [1,18], which deals with a particle cluster with the field-dependent effective length. The obtained magnetic anisotropy constants corresponding to the volume and surface contributions, intensity of the interparticle interactions, and particle size are consistent. This evidences for applicability of the model proposed in [1,18], which was previously confirmed for two-dimensional (films), for the three-dimensional ensembles of magnetic nanoparticles with the magnetic interaction.

**Acknowledgments.** Authors thanks to O.A. Bayukov and A.D. Balaev for fruitful discussions. The work was supported partially by Russian Foundation for Basic Research Grant No. 16-32-50156.



## References

[1] W.C. Nunes, L.M. Socolovsky, J.C. Denardin, F. Cebollada, A.L. Brandl, M. Knobel, Role of magnetic interparticle coupling on the field dependence of the superparamagnetic relaxation time, Phys. Rev. B - Condens. Matter Mater. Phys. 72 (2005) 1–4. doi:10.1103/PhysRevB.72.212413.

[2] E. V Dmitrienko, I.A. Pyshnaya, O.N. Martyanov, D. V Pyshnyi, Molecularly imprinted polymers for biomedical and biotechnological applications, Russ. Chem. Rev. 85 (2016) 513–536. doi:10.1070/RCR4542.

[3] S. ichi Ohkoshi, A. Namai, M. Yoshikiyo, K. Imoto, K. Tamazaki, K. Matsuno, O. Inoue, T. Ide, K. Masada, M. Goto, T. Goto, T. Yoshida, T. Miyazaki, Multimetal-Substituted Epsilon-Iron Oxide e-Ga0.31Ti0.05Co0.05Fe1.59O3 for Next-Generation Magnetic

Recording Tape in the Big-Data Era, Angew. Chemie - Int. Ed. 8506 (2016) 1–5. doi:10.1002/anie.201604647.

[4] D.A. Balaev, S.S. Yakushkin, A.A. Dubrovskii, G.A. Bukhtiyarova, K.A. Shaikhutdinov, O.N. Martyanov, Study of the high-coercivity material based on ε-Fe2O3 nanoparticles in the silica gel matrix, Tech. Phys. Lett. 42 (2016) 347–350. doi:10.1134/S1063785016040039.

[5] D.A. Balaev, A.A. Dubrovskiy, K.A. Shaykhutdinov, O.A. Bayukov, S.S. Yakushkin, G.A. Bukhtiyarova, O.N. Martyanov, Surface effects and magnetic ordering in few-nanometer-sized ε-Fe2O3 particles, J. Appl. Phys. 114 (2013) 163911. doi:10.1063/1.4827839.

[6] D.A. Balaev, I.S. Poperechny, A.A. Krasikov, K.A. Shaikhutdinov, A.A. Dubrovskiy, S.I. Popkov, A.D. Balaev, S.S. Yakushkin, G.A. Bukhtiyarova, O.N. Martyanov, Y.L. Raikher, Dynamic magnetization of ε-Fe2O3 in pulse field: Evidence of surface effect, J. Appl. Phys. 117 (2015) 1–7. doi:10.1063/1.4907586.

[7] S.S. Yakushkin, A.A. Dubrovskiy, D.A. Balaev, K.A. Shaykhutdinov, G.A. Bukhtiyarova, O.N. Martyanov, Magnetic properties of few nanometers ε-Fe2O3 nanoparticles supported on the silica, J. Appl. Phys. 111 (2012) 44312. doi:10.1063/1.3686647.

[8] O.N. Martyanov, V.F. Yudanov, Formation of disperse ferromagnetic nanoparticles in zeolites in the course of thermal activation in oxygen, J. Struct. Chem. 49 (2008) 421–426. doi:10.1007/s10947-008-0060-1.

[9] G.A. Bukhtiyarova, M.A. Shuvaeva, O.A. Bayukov, S.S. Yakushkin, O.N. Martyanov, Facile synthesis of nanosized ε-Fe2O3 particles on the silica support, J. Nanoparticle Res. 13 (2011) 5527–5534. doi:10.1007/s11051-011-0542-5.

[10] M.A. Shuvaeva, I. V. Delii, O.N. Mart'yanov, O.A. Bayukov, E.I. Osetrov, A.A. Saraev, V. V. Kaichev, N.S. Sakaeva, G.A. Bukhtiyarova, Effect of calcination temperature on the physicochemical and catalytic properties of FeSO4/SiO2 in hydrogen sulfide oxidation, Kinet. Catal. 52 (2011) 896–906. doi:10.1134/S0023158411060206.

[11] A.D. Arelaro, A.L. Brandl, E. Lima, L.F. Gamarra, G.E.S. Brito, W.M. Pontuschka, G.F. Goya, Interparticle interactions and surface contribution to the effective anisotropy in biocompatible iron oxide nanoparticles used for contrast agents, J. Appl. Phys. 97 (2005) 8–11. doi:10.1063/1.1853931.

[12] J.C. Denardin, A.L. Brandl, M. Knobel, P. Panissod, A.B. Pakhomov, H. Liu, X.X. Zhang, Thermoremanence and zero-field-cooled/field-cooled magnetization study of Cox(SiO2)1-x granular films, Phys. Rev. B. 65 (2002) 64422. doi:10.1103/PhysRevB.65.064422.

[13] K. Nadeem, H. Krenn, T. Traussnig, R. Würschum, D. V. Szabó, I. Letofsky-Papst, Effect of dipolar and exchange interactions on magnetic blocking of maghemite nanoparticles, J. Magn. Magn. Mater. 323 (2011) 1998–2004. doi:10.1016/j.jmmm.2011.02.041.

[14] V. Russier, Blocking temperature of interacting magnetic nanoparticles with uniaxial and cubic anisotropies from Monte Carlo simulations, J. Magn. Magn. Mater. 409 (2016) 50–55. doi:10.1016/j.jmmm.2016.02.070.

[15] O.N. Martyanov, R.N. Lee, V.F. Yudanov, Manifestation of granular structure in FMR spectra, J. Magn. Magn. Mater. 267 (2003) 13–18. doi:10.1016/S0304-8853(03)00296-8.

[16] O.N. Martyanov, S.N. Trukhan, V.F. Yudanov, Ferromagnetic resonance fine structure of dispersed magnets: Physical origin and applications, Appl. Magn. Reson. 33 (2008) 57–71. doi:10.1007/s00723-008-0056-1.

[17] S.N. Trukhan, O.N. Martyanov, V.F. Yudanov, Stepwise magnetization of dispersed ferromagnets due to magnetic interparticle interactions, Phys. Solid State. 50 (2008) 456–462. doi:10.1007/s11451-008-3010-z.

[18] M. Knobel, W.C. Nunes, H. Winnischofer, T.C.R. Rocha, L.M. Socolovsky, C.L. Mayorga, D. Zanchet, Effects of magnetic interparticle coupling on the blocking temperature of ferromagnetic nanoparticle arrays, J. Non. Cryst. Solids. 353 (2007) 743–

747. doi:10.1016/j.jnoncrysol.2006.12.037.
[19] P. Allia, G. Barrera, P. Tiberto, T. Nardi, Y. Leterrier, M. Sangermano, Fe3O4nanoparticles and nanocomposites with potential application in biomedicine and in communication technologies: Nanoparticle aggregation, interaction, and effective magnetic anisotropy, J. Appl. Phys. 116 (2014). doi:10.1063/1.4895837.
[20] G.F. Goya, T.S. Berquó, F.C. Fonseca, M.P. Morales, Static and dynamic magnetic properties of spherical magnetite nanoparticles, J. Appl. Phys. 94 (2003) 3520–3528. doi:10.1063/1.1599959.
[21] G.C. Papaefthymiou, E. Devlin, A. Simopoulos, D.K. Yi, S.N. Riduan, S.S. Lee, J.Y. Ying, Interparticle interactions in magnetic core/shell nanoarchitectures, Phys. Rev. B - Condens. Matter Mater. Phys. 80 (2009) 1–10. doi:10.1103/PhysRevB.80.024406.
[22] A.M. Pereira, C. Pereira, A.S. Silva, D.S. Schmool, C. Freire, J.-M. Grenèche, J.P. Araújo, Unravelling the effect of interparticle interactions and surface spin canting in γ-Fe2O3@SiO2 superparamagnetic nanoparticles, J. Appl. Phys. 109 (2011) 114319. doi:10.1063/1.3583652.
[23] V.L. Kirillov, D.A. Balaev, S. V. Semenov, K.A. Shaikhutdinov, O.N. Martyanov, Size control in the formation of magnetite nanoparticles in the presence of citrate ions, Mater. Chem. Phys. 145 (2014) 75–81. doi:10.1016/j.matchemphys.2014.01.036.
[24] R. Berger, J. Kliava, J.C. Bissey, V. Baietto, Magnetic resonance of superparamagnetic iron-containing nanoparticles in annealed glass, J. Appl. Phys. 87 (2000) 7389–7396. doi:10.1063/1.372998.
[25] C.-R. Lin, R.-K. Chiang, J.-S. Wang, T.-W. Sung, Magnetic properties of monodisperse iron oxide nanoparticles, J. Appl. Phys. 99 (2006) 08N710. doi:10.1063/1.2172891.
[26] B.D. Cullity, Introduction to Magnetic Materials, 2–nd ed., Addison-Wesley, New-York, 1972.
[27] R. Alben, J.J. Becker, M.C. Chi, Random anisotropy in amorphous ferromagnets, J. Appl. Phys. 49 (1978) 1653–1658. doi:10.1063/1.324881.

Highlights

- The interparticle interactions affect superparamagnetic behavior of nanoparticles;
- Effective magnetic anisotropy constant depends on interparticle interaction energy;
- Modified random anisotropy model was used for 3-D dispersed nanoparticles ensemble.